



BRAIN EMOTIONAL LEARNING BASED INTELLIGENT CONTROLLER FOR INDUCTION HEATING SYSTEMS

ARIJIT CHAKRABARTI¹, PRADIP KUMAR SADHU², AVIJIT CHAKRABORTY², PALASH PAL³

Keywords: Amygdala, Brain emotional learning based intelligent controller (BELBIC), Cognitive, Full bridge resonant inverter, Proportional-integral-derivative (PID), Induction heating, Zero-voltage-switching (ZVS).

This paper proposes leveraging an intelligent control strategy for controlling the power of industrial induction heating systems with series resonant inverters. Brain emotional learning based intelligent controller (BELBIC) is the proposed intelligent controller. It is based on the model of amygdala-orbitofrontal system of mammals, which is a region in brain responsible for emotional learning process. The paper also compares the performance of BELBIC with that of the conventional PID controller for induction heating systems to illustrate the performance of this control strategy. System modeling and controller simulation have been accomplished through MATLAB/ SIMULINK.

1. INTRODUCTION

Induction heating has been emerging as one of the preferred heating technologies in domestic, industrial, and medical applications these days [1]. It uses power semiconductor devices with high-frequency switching [2, 3]. The advancement in domestic and industrial induction heating technologies demands efficient control algorithms and strategies that are capable of providing robust performance against induction load variations. Over the last few years, induction heating has been focusing on development of control strategies by applying high switching frequencies with series resonant inverters, parallel quasi resonant inverters to eliminate the switching loss of semiconductor devices through soft switching, *viz.*, zero current switching (ZCS) or zero-voltage-switching (ZVS) [4, 5].

The output power of the inverters is controlled through various control schemes. The proportional-integral-derivative (PID) controller is used in induction heating systems widely. PID controllers are tuned mostly based on small amount of information about the dynamic behavior of the systems and sometimes do not provide good tuning which results in poor control. Thus, to control the power of the induction heating systems more effectively, an intelligent controller has been analyzed.

Researchers in cognitive science and artificial intelligence have developed models to simulate the processes that are involved in human intelligence leading to bio-inspired algorithm development to replicate human intelligence [6]. Moren and Balkenius introduced brain emotional learning (BEL), the computational model of emotional learning in mammalian limbic system. Lucas et al. introduced a novel intelligent controller called brain emotional learning based intelligent controller (BELBIC) that comprises the BEL model [7]. BELBIC is being utilized in various control problems like speech emotion recognition [8], emotional control of inverted pendulum, intelligent controller applied to permanent magnet synchronous machine drive [9], speed control of induction motors [10], etc. In such applications the BEL controller resulted in on-line adaptability, robustness and small computational cost. Most of the induction heating systems use PID controllers in their controlling units. Such controllers result in higher overshoots, longer settling times, etc. leading to difficulties in designing and stabilizing the

system. Previous research in other areas has shown that BEL controllers lead to good stability, strong robustness and small computational cost [8–10]. However, there is no research on BELBIC for induction heating systems, so the feasibility and performance of BELBIC with induction heating systems have not been explored yet. So BELBIC or the BEL controller has been selected here as the intelligent control strategy for power control in induction heating systems. This paper aims at studying the feasibility and evaluating the performance of BELBIC with induction heating systems. The paper also contributes towards the comparative analysis of BEL controller with a conventional PID controller. The controllers have been designed and tuned using MATLAB/SIMULINK.

The paper is organized into the sections that follow. Section 2 describes the system modelling of the induction heating system. Section 3 covers the design of the controllers. Section 4 discusses about the simulation and results. Finally, this paper is concluded in Section 5.

2. SYSTEM MODELLING

The prototype of an induction heating system is shown in Fig. 1. The main power source supplies energy to induction coil. The ac input voltage is usually rectified by the uncontrolled rectifier having four diodes and it converts an alternating current (ac) to the direct current (dc). This direct current gets filtered by the dc link capacitor and is fed to the resonant inverter. The induction coil generates an alternating magnetic field after receiving high-frequency current from the inverter and the field induces eddy currents and causes hysteresis effect to heat up the work-piece. Figure 2 shows the load circuit which comprises the work-piece and coil modeled as a transformer with a single turn secondary winding with an equivalent circuit consisting of a resistor R_e and an inductor L_e . Different parameters such as shape of the coil, diverse work-piece materials, spacing between induction coil and work-piece, temperature, excitation frequency, etc. may result in variations in equivalent load.

¹Indian Institute of Technology (ISM), Department of Electrical Engineering, Dhanbad, India, E-mail: a.chakra2010@gmail.com

²Indian Institute of Technology (ISM), Department of Electrical Engineering, Dhanbad - 826004, Jharkhand, India

³Govt. Engineering College, Techno India Dumka, Dumka-814101, Jharkhand, India

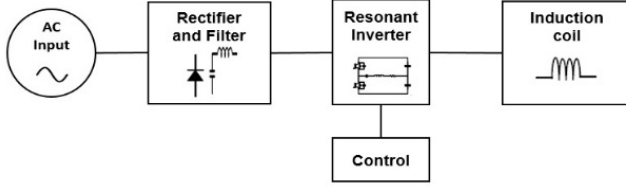


Fig. 1 – Prototype of an induction heating system.

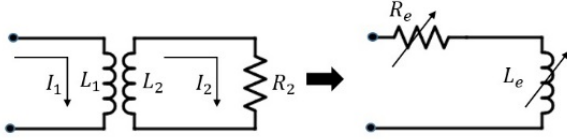


Fig. 2 – Equivalent circuit of the load.

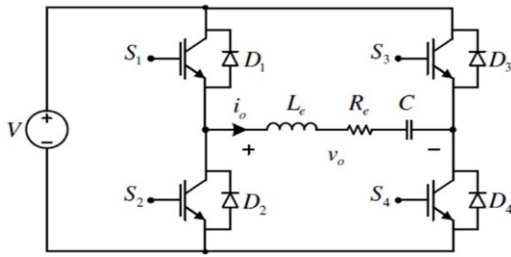


Fig. 3 – Full bridge resonant inverter for induction heating system.

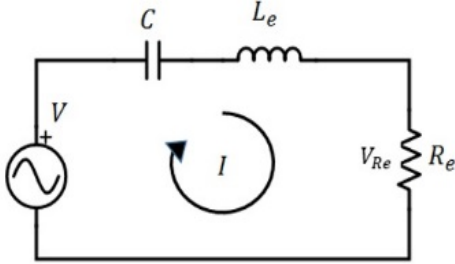


Fig. 4 – Simplified inverter circuit.

A full bridge resonant inverter with series resonant circuit has been considered for the induction heating system to be studied in this paper since it is popular and offers more control options [11]. A serially compensated inverter topology is shown in Fig. 3. It comprises four IGBTs as controllable switches (S_1 to S_4) with ultrafast anti-parallel soft recovery diodes (D_1 to D_4) and a series resonant circuit load with equivalent inductor (L_e), resistor (R_e) and resonant capacitor (C). The topology is fed by a voltage source V which can be variable or fixed. The switches are operated at a high switching frequency with switching period T_s . The series resonant circuit load represents an inductive load in this case. Figure 4 shows the simplified inverter circuit. It will be considered to calculate the voltage transfer function since it is related to the power injected to the heating system directly.

Applying Kirchhoff's law to the circuit of Fig. 4 and taking the Laplace transform, we find the following

$$V(s) - \frac{I(s)}{sC} - sL_e I(s) - R_e I(s) = 0 \quad (1)$$

$$V_{Re}(s) = R_e I(s). \quad (2)$$

From (1) and (2) we get the following equation

$$V_{Re}(s) = \frac{\frac{sR_e}{L_e}}{s^2 + \frac{sR_e}{L_e} + \frac{1}{L_e C}} V(s). \quad (3)$$

The roots of the denominator of (3) are expressed as

$$s = -\frac{R_e}{2L_e} \pm \sqrt{\left(\frac{R_e}{2L_e}\right)^2 - \frac{1}{L_e C}}. \quad (4)$$

The system will have an oscillatory (under-damped) response as the control system locks it to this natural frequency. So, the roots must be complex and should meet the condition in (5).

$$\left(\frac{R_e}{2L_e}\right)^2 < \frac{1}{L_e C}. \quad (5)$$

Under this condition, (3) can be expressed as

$$V_{Re}(s) = \frac{\frac{sR_e}{L_e}}{\left((s + \alpha)^2 + \omega^2\right)} V(s), \quad (6)$$

where

$$\alpha = \frac{R_e}{2L_e} \quad (7)$$

$$j\omega = \sqrt{\left(\frac{R_e}{2L_e}\right)^2 - \frac{1}{L_e C}}. \quad (8)$$

The voltage transfer function is given by (9):

$$\frac{V_{Re}(s)}{V(s)} = \frac{\frac{sR_e}{L_e}}{\left((s + \alpha)^2 + \omega^2\right)}. \quad (9)$$

The quality factor (Q), angular resonant frequency (ω_r) are expressed as

$$Q = \frac{\omega_r L_e}{R_e}, \quad (10)$$

$$\omega_r = \frac{1}{\sqrt{L_e C}}. \quad (11)$$

The series CLR circuit acts as a filter which will eliminate the impact of all the harmonics except the first one, so only the first harmonic will be considered for analysis. Thus the source voltage can be defined as

$$V(t) = V_i \sin \omega' t, \quad (12)$$

here V_i is the source peak voltage and ω' is the angular frequency. In frequency domain we get (13)

$$V(s) = V_i \frac{\omega'}{(s^2 + \omega'^2)}. \quad (13)$$

The voltage across resistance R_e can be used as the system variable for controlling the heat over the load. Equation (6) will result in (14) after we use (13)

$$V_{Re}(s) = \frac{s\omega' \frac{R_e}{L_e}}{\left((s+\alpha)^2 + \omega^2\right)\left(s^2 + \omega'^2\right)} V_i. \quad (14)$$

$V(t)$ is going to provide the energy to compensate the energy dissipated in the resistor. The generated heat has a linear relation with the power injected to the load. In order that the oscillations don't damp out and the controller operates around resonant frequency as the system is driven to resonance, we must have $\omega = \omega'$. As a result, the switching loss is zero because the current through the switches is zero at resonant frequency. So (14) can be written as

$$V_{Re}(s) = \frac{s\omega \frac{R_e}{L_e}}{\left((s+\alpha)^2 + \omega^2\right)\left(s^2 + \omega^2\right)} V_i. \quad (15)$$

Doing the partial fractions expansion of (15) and taking inverse Laplace transform, we get (16).

$$V_{Re}(t) = V_i \left[\frac{2}{(\alpha^2 + 4\omega^2)} \left[\alpha(1 - \omega e^{-\alpha t}) \cos \omega t + (2\omega^2 - (\alpha^2 + 2\omega^2)) e^{-\alpha t} \sin \omega t \right] \right]. \quad (16)$$

Now (16) includes the oscillatory and exponential parts. The oscillatory part will contribute to steady state response whereas the exponential part to transient response. The power is proportional to square of the peak voltage that can be obtained from the envelope function represented by (17). So (17) will contribute to the transient response and will lead to transfer function calculation.

$$V_{Re}(t) = V_i \left[\frac{2}{(\alpha^2 + 4\omega^2)} \left[\alpha(1 - \omega e^{-\alpha t}) + 2\omega^2 - (\alpha^2 + 2\omega^2) e^{-\alpha t} \right] \right]. \quad (17)$$

Arranging the terms of (17) and factorizing it we find

$$V_{Re}(t) = V_i \left[\frac{2(\alpha + 2\omega^2)}{(\alpha^2 + 4\omega^2)} \left[1 - \frac{(\alpha^2 + \alpha\omega + 2\omega^2)}{(\alpha + 2\omega^2)} e^{-\alpha t} \right] \right]. \quad (18)$$

Equation (18) can be expressed as

$$V_{Re}(t) = V_i \beta_{v1} (1 - \beta_{v2} e^{-\alpha t}), \quad (19)$$

where

$$\beta_{v1} = \frac{2(\alpha + 2\omega^2)}{(\alpha^2 + 4\omega^2)} \quad (20)$$

$$\beta_{v2} = \frac{(\alpha^2 + \alpha\omega + 2\omega^2)}{(\alpha + 2\omega^2)}. \quad (21)$$

Now power is given by (22) and (23).

$$W(t) = \frac{V_{Re}^2(t)}{R_e} \quad (22)$$

$$W(t) = V_i^2 \frac{\beta_{v1}^2}{2R_e} \left(1 - 2\beta_{v2} e^{-\alpha t} + \beta_{v2} e^{-2\alpha t} \right). \quad (23)$$

The Laplace transform of (23) results in (24).

$$W(s) = V_i^2 \frac{\beta_{v1}^2}{2R_e} \times \left(\frac{(\beta_{v2}^2 - 2\beta_{v2} + 1)s^2 + (3 - 4\beta_{v2} + \beta_{v2}^2)\alpha s + 2\alpha^2}{s^3 + 3\alpha s^2 + 2\alpha^2 s} \right) \quad (24)$$

Equation (24) expresses the power over the load as a response to a step $u(s) = 1/s$.

Hence the plant's transfer function will become

$$P(s) = sW(s) \quad (25)$$

$$P(s) = V_i^2 \frac{\beta_{v1}^2}{2R_e} \left(\frac{(\beta_{v2}^2 - 2\beta_{v2} + 1)s^2 + (3 - 4\beta_{v2} + \beta_{v2}^2)\alpha s + 2\alpha^2}{s^2 + 3\alpha s + 2\alpha^2} \right). \quad (26)$$

The transfer function in (26) provides the system information required to design the control strategy. The controller will be designed using $P(s)$.

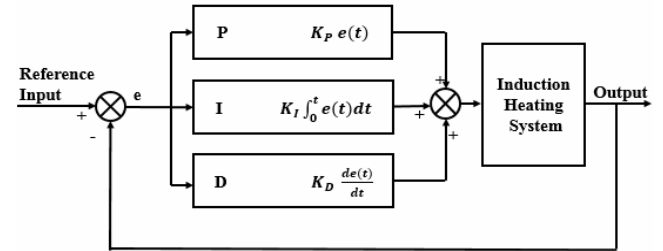


Fig. 5 – Typical PID controller.

3. CONTROLLER DESIGN

3.1. PID CONTROLLER

The proportional-integral-derivative (PID) controller is a feedback controller which drives the plant (induction heating system) to be controlled by a weighted sum of the error (difference between the output and desired set point) and makes the plant less sensitive to changes in surrounding environment and small changes in the plant [12].

Figure 5 represents the PID controller, a widely used controller, which is used for improving the dynamic response and for reducing the steady state error of the induction heating system. The derivative controller will add a finite zero to open loop plant transfer function and will improve the transient response. The integral controller will add a pole at the origin to increase system type by one through reduction of steady state error to a step function to zero. The PID controller consists of proportional, integral and derivative controls with the output given in (27).

$$u_1(t) = \left[K_P e(t) + K_I \int_0^t e(t) dt + K_D \frac{de(t)}{dt} \right]. \quad (27)$$

Here K_P , K_I and K_D are proportional, integral and derivative gains [17]. For designing the PID controller, a set of K_P , K_I , K_D is determined that improves the transient response of a system by overshoot reduction and decrease in settling time. The transfer function of the PID controller can be written as

$$C(s) = \left[K_P + \frac{K_I}{s} + sK_D \right]. \quad (28)$$

For the induction heating system, the PID parameters, viz., K_P , K_I , K_D are tuned using pid-tuning functionality of MATLAB/SIMULINK.

3.2. BRAIN EMOTIONAL LEARNING BASED INTELLIGENT CONTROLLER (BELBIC)

Bio-inspired intelligent computing is applied these days to solve various complex problems [13, 15]. The learning capability makes the intelligent methods superior in terms of adaptability. Cognitive studies include modelling, describing memory and emotion in animals and these cognitive studies are based on contemporary artificial intelligence (AI) philosophy that emphasizes on thinking and acting humanly [16]. Brain emotional learning (BEL) model was developed by Balkenius and Moren in 2001 as a computational model that mimics the amygdala, orbitofrontal cortex (OFC), Thalamus, and Sensory input cortex responsible for emotional learning and processing [14].

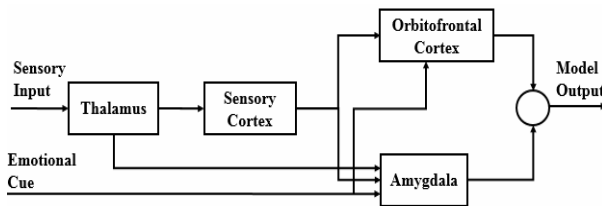


Fig. 6 – BEL model.

Based on the BEL model, Lucas *et al.* (2004) introduced the brain emotional learning based intelligent controller (BELBIC) which can be used for direct adaptive feedback control. BELBIC is basically an action-generation system based on sensory inputs and emotional cues (reward/punishment signal) [7]. It is also known as the BEL controller. Figure 6 illustrates the BEL model.

Thalamus is simply the model of real thalamus of human brain. In thalamus, pre-processing on sensory input signals like noise reduction, filtering are done. Sensory cortex receives the inputs from thalamus, and this part is responsible for subdividing and discrimination of coarse inputs from thalamus. OFC will inhibit inappropriate responses from amygdala based on the context given by the hippocampus. Amygdala, a small structure in the medial temporal lobe of brain, is responsible for emotional evaluation of stimuli. This evaluation is used as the basis for emotional states and emotional reactions. It is leveraged for attention signal and laying down long-term memories.

BELBIC gets sensory input signals through thalamus. After preprocessing on sensory input, processed input signal is sent to amygdala and sensory cortex [8]. Amygdala and OFC compute the outputs based on emotional signal received from environment. Final output is calculated by subtracting

amygdala's output from OFC's output. The thalamic connection can be calculated as the maximum overall sensory input S and this is nothing but another input to amygdala. Unlike other inputs to amygdala, the thalamic input is not projected into the orbitofrontal part and cannot be inhibited by itself.

BELBIC structure is shown in Fig. 7. The vector S represents stimuli inputs to the system. The output of each node in amygdala A_j is obtained by multiplying j^{th} input S_j with corresponding weight V_j (amygdala adaptive gain for node j) as given by

$$A_j = S_j V_j. \quad (29)$$

Similarly, the output of each node in orbitofrontal cortex O_j is obtained by multiplying j^{th} input S_j with corresponding weight W_j (OFC adaptive gain for node j) as given by

$$O_j = S_j W_j. \quad (30)$$

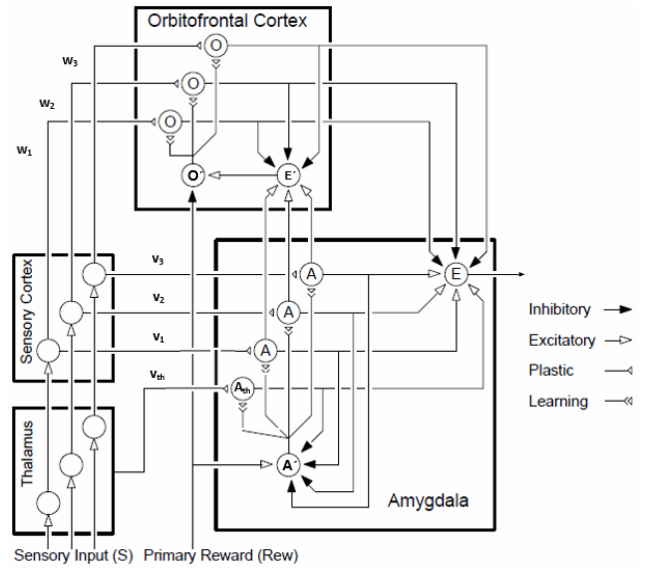


Fig. 7 – Structure of BELBIC.

If multiple sensory inputs are needed for controller design, thalamus output will be maximum of those sensory inputs, else single sensory input will directly be sent to amygdala. The thalamic connection is determined as the maximum over all stimuli S and it is another input to the amygdaloidal part. If A_{th} is the input to the amygdala part which is the maximum of stimuli inputs S and V_{th} is the corresponding amygdala adaptive gain, then we can write

$$S_{th} = \max(S_j) \quad (31)$$

$$A_{th} = S_{th} V_{th}. \quad (32)$$

BELBIC parameters are divided into two different groups, viz., the learning rates in amygdala and OFC; and the coefficients that appear in sensory input and primary reward signal formulation. The reward function Rwd is selected with the objective of minimizing the difference between the *desired* and *measured* signals. This function plays a vital role in BELBIC and it tends to increase the reward, minimizing the sensory input.

The learning rule of amygdala can be expressed as

$$\Delta V_j = a \left(S_j \max \left(0, Rwd - \sum_j A_j \right) \right). \quad (33)$$

Here a is the amygdala learning rate, ΔV_j the variation of V_j and Rwd the reinforcing (reward) signal. The weights V_j will not decrease since once an emotional reaction is learned it should not change. It is the task of OFC part to inhibit the reaction when it is inappropriate. Similarly, the learning rule in OFC can be expressed as

$$\Delta W_j = b S_j \left(\sum_j A_j - \sum_j O_j - Rwd \right). \quad (34)$$

Here b is the orbitofrontal learning rate. The A nodes generate their outputs proportionally to their contribution in predicting the reward or stress signal, while the O nodes inhibit the output of E when required. The feedback element E' is defined as the subtraction of OFC inhibitory outputs (O_j) from the summation of Amygdala nodes (A_j) excluding the A_{th} node.

$$E' = \sum_j A_j - \sum_j O_j. \quad (35)$$

The E node simply sums outputs from the A nodes and then subtracts the inhibitory outputs from O nodes. The output E of the closed-loop emotional controller is obtained from (36).

$$E = E' + A_{th}. \quad (36)$$

Architecture of BEL controller or BELBIC is shown in Fig. 8. Amygdala acts as an actuator and OFC a preventer.

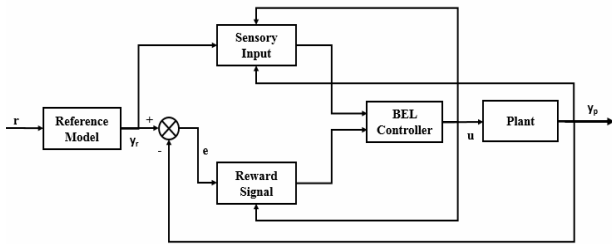


Fig. 8 – BEL controller.

The sensory input and reward signal can be arbitrary functions of reference output y_r , controller output u , error signal e , and the plant (induction heating system) output y_p . BELBIC has only one output, so for systems with multiple control inputs need one BELBIC for each control input.

Emotional cue (primary reward) and sensory inputs can be expressed as

$$Rwd = F_1(S_j, e, y_p), \quad (37)$$

$$S_j = F_2(u, e, y_p, y_r). \quad (38)$$

In this paper, the functions F_1 and F_2 are given by

$$Rwd = K_{r1}e + K_{r2} \int e dt + K_{r3} \frac{de}{dt}, \quad (39)$$

$$S_j = K_{sj}|e|, \quad (40)$$

where K_{r1} , K_{r2} , K_{r3} and K_{sj} constitute the controller parameters along with the learning rate constants (a and b), which characterize the controlled dynamic system behavior. The BELBIC obtains maximum reward when the sensory input, *i.e.*, the error signal is minimum.

A controller will be robust if it tolerates certain amount of change in the process parameters without driving the feedback system towards instability. In order to increase the robustness and improve system performance, the tuning strategy aims at minimizing a suitably identified cost function in time domain. The system performance is indicated by the cost functions expressed below [18]:

a. Integral squared error (ISE):

$$J_{ISE} = \int_0^{\infty} e^2(t) dt.$$

b. Integral absolute error (IAE):

$$J_{IAE} = \int_0^{\infty} |e(t)| dt.$$

c. Integral time-weighted squared error (ITSE):

$$J_{ITSE} = \int_0^{\infty} te^2(t) dt.$$

d. Integral time-weighted absolute error (ITAE):

$$J_{ITAE} = \int_0^{\infty} t|e(t)| dt.$$

The BELBIC parameterization is one of the current challenges confronting such a novel control structure. The BEL controller for the induction heating system is designed through finding an optimal solution set for which the cost functions are minimal through simulation using MATLAB/SIMULINK.

Table 1

Simulation parameters

Parameters	Values
R_e [Ω]	2
L_e [μ H]	47
C [μ F]	0.47
f_r [Hz]	33880
f_s [Hz]	35000
V [V]	230

Table 2

PID controller parameters

Controller parameters	Values
K_P	1.0×10^{-4}
K_I	2.0
K_D	9.0×10^{-10}

Table 3

BELBIC parameters

Learning rates		Sensory input function (S_j)	Reward function (Rwd)		
a	b	K_{sj}	K_{r1}	K_{r2}	K_{r3}
0.53	0.81	2×10^{-3}	7×10^{-3}	5×10^{-6}	4×10^{-5}

4. SIMULATION RESULTS AND DISCUSSION

Performances of the conventional PID controller and BELBIC have been simulated, analyzed and compared for the induction heating systems with full bridge series resonant inverter. The specifications and circuit parameters for the design are mentioned in Table 1, where R_e is the equivalent resistance, L_e the equivalent inductance, C the capacitance, f_r the frequency at resonance, f_s the switching frequency and V the inverter input voltage. MATLAB/SIMULINK blocks are used to design and tune the controllers.

The PID controller parameters obtained through simulation and suitable for closed loop feedback operations on induction heating systems, are mentioned in Table 2. Table 3 shows the BELBIC parameters suitable for closed loop feedback operations on induction heating systems.

Figure 9 displays the step response for the closed loop induction heating system with PID controller, whereas Fig. 10 displays the step response for the closed loop induction heating system with BELBIC.

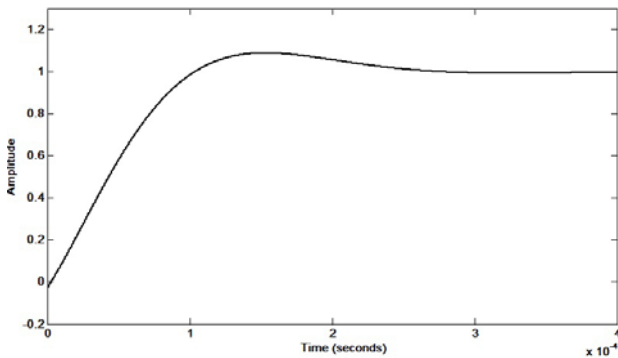


Fig. 9 – Step response of the induction heating system with PID controller.

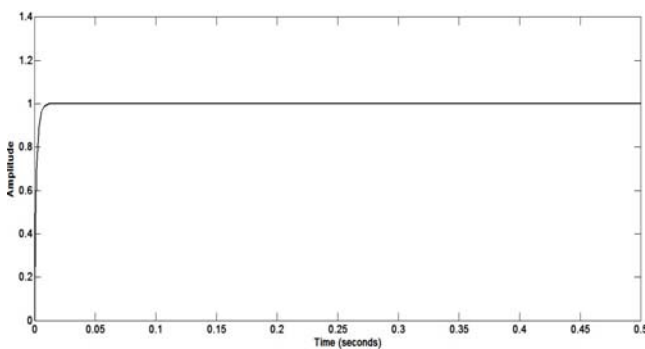


Fig. 10 – Step response of the induction heating system with BELBIC.

Table 4

Performance parameters for PID controller and BELBIC

Controller type	Overshoot M_p (%)	Rise time t_r (seconds)	Settling time t_s (seconds)
PID	1.49	9×10^{-3}	0.0245
BELBIC	0	2×10^{-5}	0.0012

Table 5

Performance indices of PID controller and BELBIC

Performance index	PID controller	BELBIC
ISE	3.20×10^{-5}	2.28×10^{-6}
IAE	5.48×10^{-5}	2.81×10^{-5}
ITSE	3.20×10^{-5}	2.57×10^{-6}
ITAE	5.48×10^{-5}	7.59×10^{-5}

The performance parameters such as overshoot, rise time, settling time for the induction heating system with PID and BEL controllers are mentioned in Table 4. Table 5 shows the values of ISE, IAE, ITSE, and ITAE for both the controllers. The comparison gives an idea of the robustness of the controller. From Table 4, it is found that the overshoot is 1.49 % with the PID controller, while the overshoot is eliminated with BELBIC. The step response rises faster and settles faster for BELBIC. Thus, the BELBIC or BEL controller will eliminate the overshoot and oscillations. Hence the induction heating system can be controlled more effectively and efficiently by brain emotional learning based intelligent controller and it will help achieve the set point for desired power level rapidly.

5. CONCLUSION

This study shows that the BEL controller or the BELBIC can be used to control the output power of the induction heating systems with full bridge series resonant inverter indicating its feasibility for such systems. The closed-loop system performance has been studied for the BELBIC and a conventional PID controller for the same induction heating system. The BEL controller has resulted in faster response, lower overshoot, faster settling which signifies that BELBIC is more suitable for the induction heating systems and it will provide improved performance as compared to the mostly used conventional PID controllers.

Future research work may include study on applicability of this emotional intelligent control scheme to induction heating systems with other inverter topologies.

ACKNOWLEDGEMENTS

Authors are thankful to the UNIVERSITY GRANTS COMMISSION, Bahadurshah Zafar Marg, New Delhi, India for granting financial support under Major Research Project entitled “Simulation of high frequency mirror inverter for energy efficient induction heated cooking oven using PSPICE” and also grateful to the Under Secretary and Joint Secretary of UGC, India for their active co-operation.

Received on January 21, 2017

REFERENCES

- Ó. Lucía, P. Maussion, E.J. Dede, J.M. Burdío, *Induction Heating Technology and its Applications: Past Developments, Current Technology, and Future Challenges*, IEEE Transactions on Industrial Electronics, **61**, 5, pp. 2509–2520 (2014).
- A. Bhattacharya, P.K. Sadhu, A. Bhattacharya, N. Pal, *Voltage Controlled Resonant Inverter – An Essential Tool For Induction Heated Equipment*, Rev. Roum. Sci. Techn. – Électrotechn. et Énerg., **61**, 3, pp. 273–277 (2016).
- T. Leuca, Ş. Nagy, N.D. Trip, Helga Silaghi, ClaudiuMich-Vancea, *Optimal Design for Induction Heating using Genetic algorithms*, Rev. Roum. Sci. Techn. – Électrotechn. et Énerg., **60**, 2, pp. 133–142 (2015).
- A. Chakraborty, D. Roy, T.K. Nag, P.K. Sadhu and N. Pal, *Open Loop Power Control of a Two-Output Induction Heater*, Rev. Roum. Sci. Techn. – Électrotechn. et Énerg., **62**, 1, pp. 48–54 (2017).
- V.V.S.K. Bhajana, P. Drabek, M. Jara, *Performance Evaluation of LLC Resonant Full Bridge DC Converter for Auxiliary Systems in Traction*, Rev. Roum. Sci. Techn. – Électrotechn. et Énerg., **60**, 1, pp. 79–88 (2015).

6. R.R. Morphy, *Biological and Cognitive Foundations of Intelligent Sensor Fusion*, IEEE Transaction on Systems, Man and Cybernetics, **26**, 1, pp. 42–51 (1996).
7. C. Lucas, D. Shahmirzadi, N. Sheikholeslami, *Introducing BELBIC: Brain Emotional Learning Based Intelligent Control*, Intelligent Automation & Soft Computing, **10**, 1, pp. 11–21 (2004).
8. S. Motamed, S. Setayeshi, A. Rabiee, *Speech emotion recognition based on a modified brain emotional learning model*, Biologically Inspired Cognitive Architectures (Elsevier), **19**, pp. 32–38 (2017).
9. M. Qutubuddin, N. Yadaiah, *Modeling and implementation of brain emotional controller for Permanent Magnet Synchronous motor drive*, Engineering Applications of Artificial Intelligence (Elsevier), **60**, pp. 193–203 (2017).
10. E. Daryabeigi, N.R. Abjadi, G.R.A. Markadeh, *Automatic Speed Control of an Asymmetrical Six-phase Induction Motor Using Emotional Controller (BELBIC)*, Journal of Intelligent and Fuzzy Systems, **26**, 4, pp. 1879–1892 (2014).
11. H. Sarnago, Ó. Lucía, M. Pérez-Tarragona, J.M. Burdío, *Dual-Output Boost Resonant Full-Bridge Topology and its Modulation Strategies for High-Performance Induction Heating Applications*, IEEE Transactions on Industrial Electronics, **63**, 6, pp. 3554–3561 (2016).
12. X. Liu, M. Zhang, A.G. Richardson, T.H. Lucas, J.V. Spiegel, *Design of a Closed-Loop, Bidirectional Brain Machine Interface System With Energy Efficient Neural Feature Extraction and PID Control*, IEEE Transactions on Biomedical Circuits and Systems, **11**, 4, pp. 729–742 (2017).
13. N. Garmsiri, N. Sepehri, *Emotional Learning Based Position Control of Pneumatic Actuators*, Intelligent Automation and Soft Computing (Taylor and Francis), **20**, 3, pp. 433–450 (2014).
14. C. Balkenius, J. Moren, *Emotional Learning: A Computational Model of the Amygdala*, Cybernetics and Systems, **32**, 6, pp. 611–636 (2001).
15. S. Klecker, B. Hichri, P. Plapper, *Robust BELBIC-Extension for Trajectory Tracking Control*, Journal of Mechanics Engineering and Automation, **7**, 2, pp. 84–93 (2017).
16. G. Miller, *The cognitive revolution: a historical perspective*, Trends in Cognitive Sciences, **7**, 3, pp. 141–144 (2003).
17. X. Yang, C. Song, J. Sun, X. Wang, *Simulation and implementation of Adaptive Fuzzy PID*, Journal of Networks, **9**, 10, pp. 2574–2581 (2014).
18. Y.K. Soni, R. Bhatt, *BF-PSO optimized PID Controller design using ISE, IAE, IATE and MSE error criteria*, International Journal of Advanced Research in Computer Engineering & Technology (IJARCET), **2**, 7, pp. 2333–2336 (2013).